J. Fluid Mech. (1990), *vol.* 214, *pp.* 111–129
Printed in Great Britain

Formation of longitudinal vortices in the sublayer due to boundary-layer turbulence

By Y. AIHARA
Department of Aeronautics, Faculty of Engineering, University of Tokyo, Japan

(Received 31 March 1988 and in revised form 25 September 1989)

A number of experiments have indicated that the behaviour of longitudinal vortices in the sublayer of a turbulent boundary layer has a significant effect on the equilibrium of the whole flow field, but the formation of such longitudinal vortices remains unclarified. In the present paper, paying attention to the random turbulent motions normal to the wall which induce a dynamic instability causing the generation of the regular longitudinal vortices, a turbulence model is introduced to analyse the generation of the longitudinal vortices in the sublayer of a turbulent boundary layer.

By integrating the results of the analysis with previous experimental results for the behaviour of developing longitudinal vortices, a feedback loop linking regular and irregular motions in the turbulent boundary layer is presented.

It has been experimentally confirmed that even at low Reynolds number, regular longitudinal vortices are formed when a disturbance is applied to a boundary layer. As for the stability region described in terms of the intensity of the disturbance and the wavenumber of the longitudinal vortices, no conflict between analysis and experiment is observed. Using the thermodynamic argument of irreversible processes the formation of longitudinal vortices close to the wall by the turbulence in the boundary layer is shown to be physically reasonable.

1. Introduction

It has been accepted that the growth-burst process of longitudinal vortices formed in the viscous sublayer of a turbulent boundary layer on a flat plate constitutes a vital basic step to the establishment of a turbulent boundary layer (Cantwell 1981), but with respect to the particularly significant mechanism of the longitudinal vortices being generated, the solution is yet to be obtained.

The longitudinal vortices themselves do impart a stationary periodic three-dimensionality to the flow, but do not directly cause turbulence. With progressive growth of the longitudinal vortices the vortices on both sides of an upwash come closer together and form a pair, which intensifies the upwash; and as the result of an unstable velocity profile being locally generated, horseshoe vortices are formed (Blackwelder & Eckelmann 1979). There is a close resemblance between this process and the behaviour of Görtler vortices, i.e. longitudinal vortices in a boundary layer on a concave plate (Aihara & Koyama 1981*a*, 1981*b*, 1982; Swearingen & Blackwelder 1987). As stated above, in the boundary layer along a concave surface the longitudinal vortices are formed as Görtler vortices due to the primary dynamic instability, while in the turbulent boundary layer along a flat plate they are formed by unknown causes. Because of this similarity, the longitudinal vortices of a

turbulent boundary layer on a flat plate are often discussed in relation to Görtler vortices.

In this connection it is important to make clear how the same effect of the centrifugal force causing Görtler vortices to develop on a concave plate occurs on a flat plate.

Investigating the influence of the growth of a boundary layer in the analysis of the stability of longitudinal vortices on a concave plate, the present author and others have found that the existence of a positive $\partial\bar{v}/\partial x$ (where $\bar{v}$ is the component of the mean flow of a boundary layer normal to the wall and x is the streamwise coordinate) is equivalent to having a concave wall. The development of longitudinal vortices has also been experimentally verified by deliberately setting such a non-parallel flow in the boundary layer on a rough flat plate (Aihara, Tomita & Ito 1985). This finding is also pointed out by Brown & Thomas (1977), where the coherent structure of turbulence is discussed in relation to the curvature of the streamline at the edge of the boundary layer given by the second derivative of the thickness with respect to the streamwise direction. As another possibility of creating longitudinal vortices in the boundary layer on a flat plate, the generation based on the flow curvature due to an amplified two-dimensional travelling wave has also been debated (Görtler & Witting 1958; Benny & Lin 1960; Klebanoff, Tidstrom & Sargent 1962; Greenspan & Benny 1963).

Comparing these discussions with the experimentally observed behaviours of longitudinal vortices in the sublayer, it seems that these conceptions fail to explain fully the generation of longitudinal vortices in the sublayer. The longitudinal vortices resulting from the condition $\partial\bar{v}/\partial x > 0$, that is, due to the concavity of the streamline, may be equated to Görtler vortices. Meanwhile it is likely that $|\partial\bar{v}/\partial x|$ increases as the distance from the wall increases. As the axes of Görtler vortices, especially in the amplified state, will be located in the outer layer of the boundary layer, the longitudinal vortices thus formed will also be located in the outer part of the boundary layer. Then these longitudinal vortices will not persist for a long time because of the peripheral large disturbance and accordingly it is hard to presume that they will behave as structural longitudinal vortices of the sublayer.

Further, as for the generation due to amplified waves, even if an irregular two-dimensional disturbance develops in the turbulent boundary layer, such a disturbance will decay in a flow such as in the sublayer close to the wall.

Therefore the present author has decided to reconsider the problem taking the longitudinal vortices in the sublayer as a specific property of the turbulent boundary layer. Here the important points are that (i) the physics explaining that the statistical property of the random fluctuations in the turbulent boundary layer should be linked to the generation of structural longitudinal vortices, and (ii) both the turbulence and the longitudinal vortices constitute a sort of feedback system to maintain the equilibrium of a fully developed turbulent boundary layer.

2. Analysis

2.1. *Dynamic instability due to Reynolds stress and a turbulence model*

It should be noted that what is common to the generation of longitudinal vortices is that the fundamental flow possesses either centrifugal force or buoyancy as dynamic forces in the direction normal to the wall surface; and these forces bring about the dynamic instability of fluid which induces the longitudinal vortices. The condition

for such instability emerges when the dynamic force is spatially distributed such that it diminishes in its applied direction.

It is apparent that in a constant-temperature parallel laminar boundary layer on a flat plate, there is no dynamic force of either kind and accordingly there is no static pressure gradient normal to the wall surface either. For a turbulent boundary layer along a concave wall (radius of curvature r), the general equation for the time-averaged motion normal to the wall to be considered is

$$\bar{u}\frac{\partial\bar{v}}{\partial x}+\bar{v}\frac{\partial\bar{v}}{\partial y}+\frac{\partial\overline{u'v'}}{\partial x}+\frac{\partial\overline{v'^2}}{\partial y}+\frac{\bar{u}^2}{r}+\frac{\overline{u'^2}}{r}=-\frac{1}{\rho}\frac{\partial\bar{p}}{\partial y}+F+\nu_0\nabla^2\bar{v}. \tag{1}$$

It has been assumed that r is sufficiently larger than the thickness of the boundary layer, where y, ρ, p, u, v, F, and ν_0 are respectively the coordinate normal to the wall surface, constant density, static pressure, velocity in x-direction, velocity in y-direction, body force and molecular viscosity; an overbar stands for time averaging, a prime represents a fluctuation, and ∇^2 is the Laplacian operator. The dynamic instability which generates Taylor vortices (Taylor 1923) and Görtler vortices (Görtler 1940) originates from an equilibrium between $\bar{u}^2/r$ and $(-1/\rho)(\partial\bar{p}/\partial y)$, while the thermal instability (Terada 1928) arises from that between F and $(-1/\rho)(\partial\bar{p}/\partial y)$. As stated in §1, it is also understandable from (1) that $\partial\bar{v}/\partial x$ potentially contributes to the generation of longitudinal vortices. Similarly, when the third, fourth and sixth terms of (1) and the distribution of $\bar{p}$ balancing them fall into a dynamically unstable equilibrium, even on a flat plate (r: infinite) longitudinal vortices will emerge directly, caused by a disturbance within the boundary layer. In the model concerning the longitudinal vortices in the sublayer (i.e. Coles 1978), discussion about Taylor–Görtler vortices centres on the emergence of a local curvature due to changes in the flow, that is, the disturbance is considered to contribute to the formation of longitudinal vortices through the temporal concavity of the stream surface.

For a fully developed turbulent boundary layer on a flat plate, (1) can be approximated as follows:

$$\frac{\partial\overline{v'^2}}{\partial y}=-\frac{1}{\rho}\frac{\partial\bar{p}}{\partial y}+\nu_0\frac{\partial^2\bar{v}}{\partial y^2}. \tag{1}'$$

Referring to Klebanoff's experiment (1955), the conceptional diagram of the left-hand side of (1)′ will look like figure 1 and it is seen that the regions fulfilling the above-mentioned condition for dynamic instability will be the outer layer and the sublayer of the boundary layer. As indicated in figure 1 (*b*), the domain in which the dynamic force $\partial\overline{v'^2}/\partial y$ weakens in the direction of its application, is dynamically unstable and accordingly the second derivative of $\overline{v'^2}$ with respect to y is important. Figure 1 (*b*) is a schematic expression of this relationship. In the outer layer, where large-scale turbulence prevails, the growth and development of any systematic longitudinal vortices is unlikely; and therefore subsequent discussions will be confined to the instability in the sublayer and its vicinity.

It is common when discussing the turbulent boundary layer, instead of dealing directly with the Reynolds stress as in (1)′, to shift the Reynolds stress term to the right-hand side so that in the so-called turbulence model it is treated as a viscous term (Launder & Spalding 1972). To introduce this procedure, (1)′ may be re-written as follows:

$$0=-\frac{1}{\rho}\frac{\partial\bar{p}}{\partial y}+\frac{\partial}{\partial y}\left(\nu_0\frac{\partial\bar{v}}{\partial y}-\overline{v'^2}\right). \tag{2}$$

Comparison between $\overline{v'^2}$ and the molecular viscous stress $\nu_0\,\partial\bar{v}/\partial y$ shows that both of

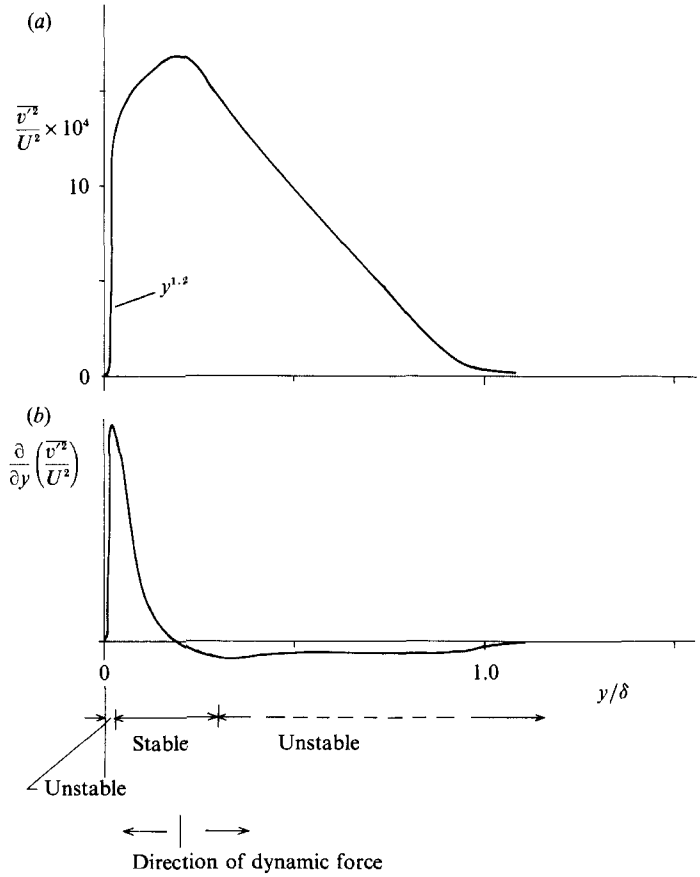

FIGURE 1. (*a*) Distribution of $\overline{v'^2}/U^2$ in the boundary layer on a flat plate, as measured by Klebanoff (1955). (*b*) Schematic figure of the distribution of dynamic force, $\partial\overline{v'^2}/\partial y$, and the stable and unstable regions in the turbulent boundary layer.

these represent mean transports of momentum in the y-direction. The form of (2) suggests the introduction of a turbulence model assuming that $\overline{v'^2}$ also depends on $\partial\bar{v}/\partial y$. The turbulence model is a mathematical hypothesis and the validity can only be verified by experimentation, but the introduction of this model will make it possible to express $\overline{v'^2}$ in terms of the mean velocity $\bar{v}$ and an unknown turbulence viscosity ν_T. As stated later the y-directional distribution of ν_T is vitally associated with generation of the longitudinal vortices in the sublayer. Thus, this model will offer one means of linking the disturbance intensity in the boundary layer to the generation of the longitudinal vortices in the sublayer. In the case of a boundary layer developing in the x-direction, $\partial\bar{v}/\partial y > 0$ is valid; therefore the introduction of $-\overline{v'^2} = \nu_T \partial\bar{v}/\partial y$ as a so-called turbulence model into (2) will make $\nu_T < 0$ valid. Thus, the problem of dynamic instability in the turbulent boundary layer will reduce to one of viscous instability with diffusion in a direction which is the reverse of that due to molecular viscosity.

Now (2) may be re-written as follows:

$$0 = -\frac{1}{\rho}\frac{\partial \bar{p}}{\partial y} + \frac{\partial}{\partial y}\left(\nu \frac{\partial \bar{v}}{\partial y}\right), \tag{3}$$

where ν is a kinematic viscosity coefficient which is equal to ν_0 on the wall surface and usually becomes a function of y as the distance from the wall increases.

Based on the above, the linear stability of longitudinal vortices will now be analysed.

2.2. *Linear stability analysis of longitudinal vortices*

The coordinates (x, y, z) are respectively orthogonal coordinates in the direction of a uniform flow from the leading edge of a two-dimensional plate, in the normal direction to the plate and in the direction parallel to the leading edge, their velocity components in respective directions being (u, v, w). With respect to the mean flow, the non-uniform static pressure $\bar{p}(y)$ and the parallel velocity $\bar{u}(y)$ will be considered, and it is supposed that on these are superposed the longitudinal vortices-induced velocity field and static pressure. Here a temporal or spatial amplification of the longitudinal vortices should be presumed. Here, considering the experimental fact that the longitudinal vortices are formed non-stationarily in the sublayer, Görtler's version based on the temporal amplification (Görtler 1940) will be taken as an analytical expression of the longitudinal vortices. Namely,

$$\left.\begin{aligned} u &= \bar{u}(y) + \tilde{u}(y)\cdot\cos\sigma z\cdot e^{\omega t},\\ v &= \tilde{v}(y)\cdot\cos\sigma z\cdot e^{\omega t},\\ w &= \tilde{w}(y)\cdot\sin\sigma z\cdot e^{\omega t},\\ p &= \bar{p}(y) + \tilde{p}(y)\cdot\cos\sigma z\cdot e^{\omega t}. \end{aligned}\right\} \tag{4}$$

where the quantities bearing ˜ are disturbance amplitude functions; and σ, ω are respectively the spatial wavenumber and the temporal amplification factor.

Next, substitution of (4) into the continuity equation and Navier–Stokes equations yields the following linear equations for disturbance due to the longitudinal vortices:

$$\frac{d\tilde{v}}{dy} + \sigma\tilde{w} = 0, \tag{5}$$

$$\omega\tilde{u} + \frac{d\bar{u}}{dy}\tilde{v} = \nu'\left(\frac{d^2\tilde{u}}{dy^2} - \sigma^2\tilde{u}\right) + \frac{d\nu'}{dy}\frac{d\tilde{u}}{dy}, \tag{6}$$

$$\omega\tilde{v} = -\frac{1}{\rho}\frac{d\tilde{p}}{dy} + \nu\left(\frac{d^2\tilde{v}}{dy^2} - \sigma^2\tilde{v}\right) + \frac{d\nu}{dy}\frac{d\tilde{v}}{dy}, \tag{7}$$

$$\omega\tilde{w} = \frac{\sigma}{\rho}\tilde{p} + \nu\left(\frac{d^2\tilde{w}}{dy^2} - \sigma^2\tilde{w}\right) + \frac{d\nu}{dy}\frac{d\tilde{w}}{dy}. \tag{8}$$

The boundary conditions are set such that the disturbance amplitude may be zero at $y = 0$ and ∞. In (7) and (8) the same kinematic viscosity coefficient ν is employed, but in (6) for x-directional motion a different ν' is adopted. This ν' is significantly affected by the correlation of turbulence velocities in the x- and y-directions, u' and v', and for its turbulence model numerous studies have been done (for instance, Launder & Spalding 1972) since Prandtl (1925). Then, as is obvious from (5)–(8), (6) is not simultaneous with the other three equations. Therefore, (6) will not be included in subsequent analyses for stability (except when $\tilde{u}$ must be found).

As shown in (3), ν is generally a function of y. According to Klebenoff's experiment (1955), at $u_\tau y/\nu_0 \leqslant 100$, $\overline{v'^2}$ is proportional to $y^{1.2}$ (figure 1). Meanwhile, $\partial\bar{v}/\partial y$ being proportional to $y^{\frac{1}{2}}$, an approximate model which assumes that ν_T is proportional to

y close to the wall will hold. Thus, for the sublayer under consideration and its vicinity, the following equation can be obtained:

$$\frac{\nu}{\nu_0} = 1 + ay, \tag{9}$$

where a is a constant. Eliminating $\tilde{w}, \tilde{p}$ from (5), (7) and (8) and employing (9) yields:

$$\left\{(1+ky)\left(\frac{\mathrm{d}^2}{\mathrm{d}y^2}-\sigma^2\right)+2k\frac{\mathrm{d}}{\mathrm{d}y}-\omega\right\}\left(\frac{\mathrm{d}^2}{\mathrm{d}y^2}-\sigma^2\right)\tilde{v} = 0. \tag{10}$$

Equation (10) is a non-dimensional equation taking the friction velocity u_τ, ν_0/u_τ and ν_0/u_τ^2 respectively as units of velocity, length and time; and $k = a\nu_0/u_\tau$.

The solution to the present problem will be given by such a relation of eigenvalues of σ, k and ω that in (10) the conditions $\tilde{v} = 0$ and $\mathrm{d}\tilde{v}/\mathrm{d}y = 0$ can be satisfied at $y = 0$ and ∞. If $\omega > 0$, i.e. the unstable domain of longitudinal vortices agrees with $k < 0$, that is, the dynamic instability due to the turbulent motion, the physics of longitudinal vortices formation stated in §2.1 will be substantiated.

First a solution to

$$\left(\frac{\mathrm{d}^2}{\mathrm{d}y^2}-\sigma^2\right)\tilde{v} = 0, \tag{11}$$

which satisfies the boundary conditions at infinity, will be given by

$$\tilde{v} = A_0\,\mathrm{e}^{-\sigma y}, \tag{12}$$

where A_0 is a constant.

Next, another solution is to be sought by the method of weighted residuals (Finlayson 1972). It is seen that among the solutions, close to the wall, to

$$\left\{(1+ky)\left(\frac{\mathrm{d}^2}{\mathrm{d}y^2}-\sigma^2\right)+2k\frac{\mathrm{d}}{\mathrm{d}y}-\omega\right\}\tilde{v} = 0, \tag{13}$$

one which satisfies the boundary conditions at infinity is

$$\tilde{v} = B_0\,\mathrm{e}^{-\lambda y}, \quad \lambda = k+(k^2+\sigma^2+\omega)^{\frac{1}{2}}, \tag{14}$$

where B_0 is a constant. Further, putting

$$\tilde{v} = (B_0+B_1 y+B_2 y^2+B_3 y^3+\ldots)\,\mathrm{e}^{-\lambda y}, \tag{15}$$

(where $B_1, B_2, \ldots$, are constants), substituting (15) into (13), and integrating it from $y = 0$ to $y = \infty$ yields an algebraic equation containing eigenvalues and $B_0, B_1, \ldots$. Similar integrations after multiplying (13) by $y, y^2, \ldots$, yield other algebraic equations. Eliminating $B_1, B_2, \ldots$, from these equations reduces (15) to:

$$\tilde{v} = B_0(1+M_1 y+M_2 y^2+M_3 y^3+\ldots)\,\mathrm{e}^{-\lambda y}, \tag{16}$$

where $M_1, M_2, \ldots$ are coefficients containing σ, k, and ω. Summation of (12) and (16) gives a solution to (10) which satisfies the boundary conditions at infinity. Then with the boundary conditions for $y = 0$ provided, the following equation can be derived as a secular equation of the ultimate eigenvalue relation:

$$\sigma+M_1-\lambda = 0. \tag{17}$$

2.3. *Results and discussion*

Equation (17), namely $F(\sigma, \omega, k) = \sigma+M_1-\lambda = 0$ is solved as follows using a computer. That is, the value of k which satisfies $F(\sigma, \omega, k) = 0$ for specific values of

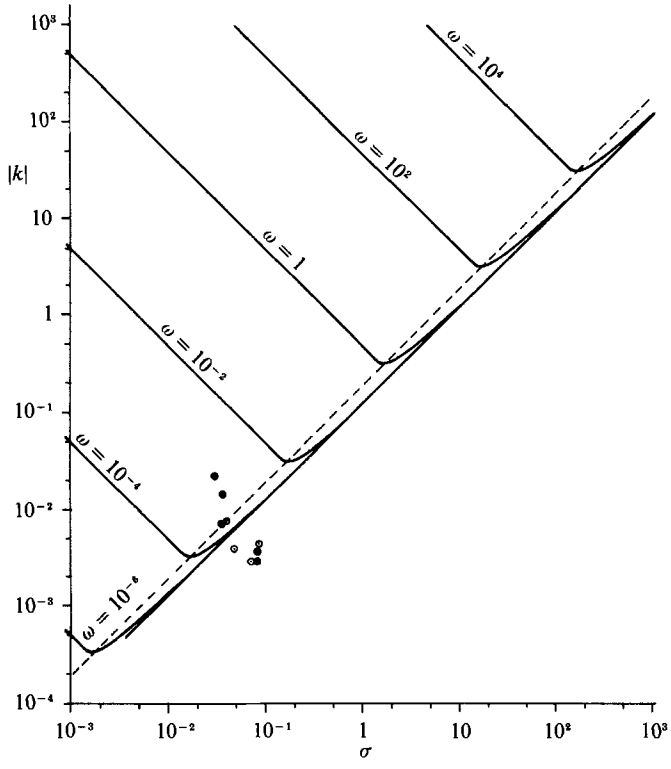

FIGURE 2. Stability diagram for longitudinal vortices near the wall. Experimental points ○ and ● are obtained for the roughness-Reynolds-number range 33.3–83.3 and 133–167, respectively.

ω and σ is found. In consequence a stability diagram as indicated in figure 2 is obtained using the first four terms in (16); k on the ordinate is negative. It is known that the longitudinal vortices will be generated in the region where the equilibrium in the y-direction in (1)′ constitutes the condition for dynamic instability.

From figure 2, it is seen that in a fully developed turbulent boundary layer, the unstable range of wavenumber for longitudinal vortices becomes wider, while in a decayed turbulent boundary layer, the wavenumber of the longitudinal vortices becomes smaller and the rate of the amplification reduces.

A broken line linking the minimum values in curves for ω = constant will provide the condition for the corresponding maximum amplification of the disturbance. Incidentally, employing Klebanoff's data (1955) of the distribution of $\overline{v'^2}$ near the wall surface based on his experiment about a fully developed turbulent boundary layer ($u_\tau y/\nu_0 \gtrsim 10, R_x = 4.2 \times 10^6$) and an experimental formula (Schlichting 1968) about a boundary layer which develops according to a one-seventh power law, the value of k is estimated at -8.7×10^2, and it is seen that the wavenumber σ of the most amplified longitudinal vortices will be of the order of 10^2 or more. This estimate is only rough since the one-seventh power law is not a good approximation for the flow in the vicinity of the wall. It is significant, however, that from this estimate it follows that in the sublayer of a developed turbulent boundary layer σ of the most amplified longitudinal vortices is large or in other words small-scale vortices are selectively amplified.

Referring to the results obtained above, the important points mentioned in §1 will be discussed below.

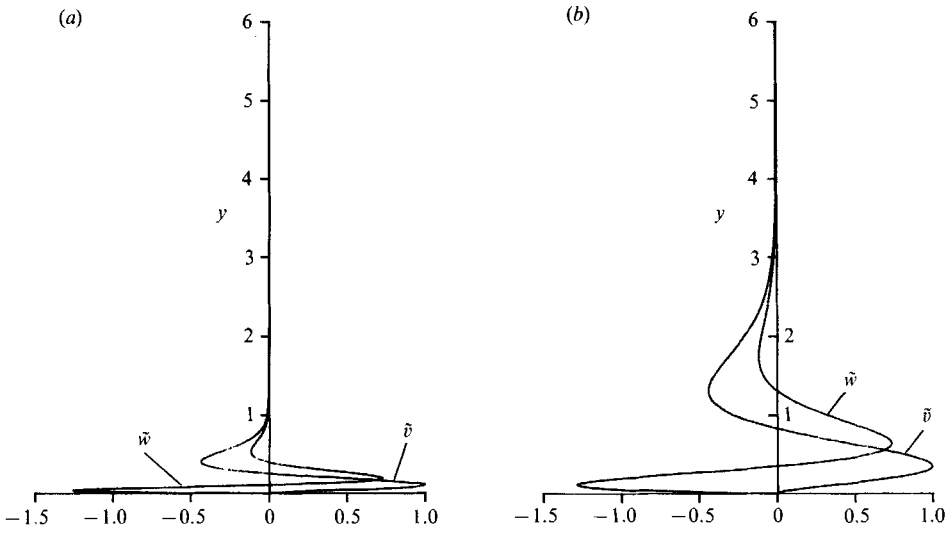

FIGURE 3. Variation of the normal and the spanwise velocity components of longitudinal vortices, $\tilde{v}$ and $\tilde{w}$, in terms of $u_\tau y/\nu_0$. (a) $\omega = 50.0$, $\sigma = 12.0$. (b) $\omega = 5.0$, $\sigma = 3.6$.

(i) The physics stated above that the statistical property of a turbulent boundary layer as represented by the y-directional distribution of $\overline{v'^2}$ produces a dynamic equilibrium expressed by (1)′. This equilibrium yields a dynamically unstable distribution in the sublayer which is quantitatively shown by the instability of longitudinal vortices at $k < 0$ in the present analysis. Through the introduction of a turbulence model which is deemed physically valid, it is deduced that the random turbulence phenomenon, as the turbulence kinematics viscosity which is a statistical property, contributes to the formation of regular longitudinal vortices. This relation will be acceptable as long as the time constant for the growth of longitudinal vortices can be considered sufficiently large as compared with the time constant for turbulence.

Distributions of $\tilde{v}$ and $\tilde{w}$ for different $|k|$ are shown in figure 3. As expected, in the case of large $|k|$, the damping due to the viscosity is large, the distributions concentrate close to the wall, whereas in the case of small $|k|$, where the coherent longitudinal vortices grow, the distributions extend from the wall. Though they have something in common, these longitudinal vortices should be distinguished from Görtler vortices.

(ii) The statistical distribution and the process of achieving the equilibrium in the turbulent boundary layer is beyond the scope of the present analysis. Namely, the present analysis gives an eigenvalue relation among the intensity of the turbulence in the existing boundary layer, the wavenumber of longitudinal vortices in the sublayer, the amplification factor, and the distribution function. It does not, however, yield any solution for the turbulence in the boundary layer. As for $\overline{v'^2}(y)$, experimentally assuming in (9) that it is proportional to y close to the wall, its coefficient is obtained as an eigenvalue k in the stability analyses. Nevertheless, by considering the behaviour of the longitudinal vortices supported by available experiments, it is possible to suggest the following feedback loop (figure 4). Namely, it is known from the obtained value of σ corresponding to large $|k|$ for a fully developed turbulent boundary layer that the wavelength of the most amplified

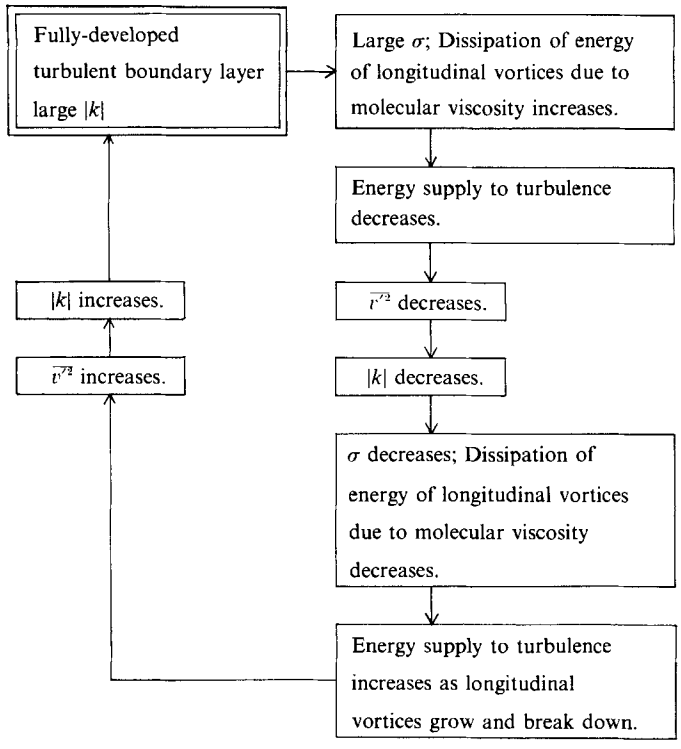

FIGURE 4. Feedback loop linking the intensity of turbulence in the boundary layer with the formation of longitudinal vortices in the sublayer.

longitudinal vortices in this state is of the order of at most one-tenth the value of ν_0/u_τ which is the scale of the sublayer thickness. Also it should be noted that the corresponding value of ω is very large. In such a condition, the rapid dissipation of energy transferred from the mean flow prevails, and the coherent structure will easily vanish under the influence of molecular viscosity. This fact implies that the contribution of the longitudinal vortices, through their growth, ejection and breakdown, to the energy supply to the turbulence (Kline *et al.* 1967; Corino & Brodkey 1969; Kim, Kline & Reynolds 1971; Willmarth & Lu 1972) diminishes, which leads to a decrease in $\overline{v'^2}$, i.e. a drop in $|k|$. With the drop in $|k|$, σ in figure 2 decreases along the dotted line and accordingly the wavelength of the amplified longitudinal vortices increases. Thus, the vortices with a wavelength of about 10–10^2 in ν_0/u_τ as experimentally observed will emerge and through their ejection and breakdown the value of $\overline{v'^2}$ increases, thereby $|k|$ increases. Such a feedback system can be considered to explain how an equilibrium is maintained between coherent motion and random turbulence in the turbulent boundary layer. It can be inferred that this process produces the fluctuation of the longitudinal vortices observed in the sublayer.

According to Rao, Narasimha & Narayanan (1971), the mean time between bursts is found to be $6\delta/U$, where U and δ are the external flow velocity and the boundary-layer thickness, respectively. The bursting interval seems to be associated with the time constant of the feedback loop suggested from the present analysis. Since it is suspected that a disturbance in the outer layer plays a vital role in the feedback

mechanism, it would be reasonable to think that the scales which represent not only the sublayer but also the boundary layer as a whole are involved in the determination of the time constant.

(iii) Further, extensively applying the results of the present analysis to a general boundary layer involving a disturbance, it may be speculated that even in the case of a laminar boundary layer involving a disturbance of small amplitude such as Tollmien–Schlichting waves there is the likelihood of longitudinal vortices being generated close to the wall surface on account of small $\overline{v'^2}$ or the accompanying small $|k|$ and the flow being three-dimensionalized.

3. Experiment

The significance of the present study lies not in the fact that the transition process of a boundary layer has been investigated through the usual harmonic analysis of small disturbances, but that a regular structural pattern of an already disturbed boundary layer is being investigated. Thus the experimental verification of the process of the formation of regular structure due to fluctuations is of great importance in the present study.

The above analysis had revealed that the distribution of $\overline{v'^2}$ in the boundary layer dominates the formation of longitudinal vortices and the Reynolds number is not directly involved. Therefore, the experiment was designed such that a random disturbance was deliberately introduced into a laminar boundary layer of low Reynolds number to create longitudinal vortices therein.

3.1. *Apparatus and procedure*

The experiment was conducted with a two-dimensional flat plate, 1000 mm long × 10 mm thick (figure 5), placed in a suction type low-turbulence wind tunnel with a cross-sectional area of the test section of 500 mm × 500 mm. For convenience of flow observation, both the test section of the wind tunnel and the flat plate were made of transparent acrylic resin. A gap of 1 mm was provided between the flat plate and the tunnel walls. The leading edge of the plate was sharpened in a wedge of 30°. At 100 mm from the leading edge there was set spanwise a two-dimensional slit which was cut at an angle of 30° to the surface, the width of the slit being 1 mm.

The measurements consisted of observations of the flow by photography from outside the test section and quantitative measurements by means of a x-probe for hot-wire anemometry attached to a three-dimensional traversing mechanism located within the test section. As the measurement of $\bar{v}$ and v' are especially important for this study, the calibration was carefully performed and the cosine law, i.e. directional characteristics of hot wire, was confirmed. As the swept angle of each wire is $\pm 30°$, the calibration was performed by changing the probe angle within $\pm 80°$ so as to confirm the cosine law between $+50°$ and $-50°$ for each wire. As a matter of fact, the measured deflection of the flow is less than 4° at the most, which is well within the calibration. The signals were processed by the computer to calculate and display the instantaneous values and statistical values of u and v spectra and other necessary quantities.

3.2. *Results and discussion*

3.2.1. *Generation of longitudinal vortices*

JIS-specified no. 60 abrasive grains were evenly sprayed spanwise over a width of 54 mm from 0.5 mm downstream of the slit. The diameters of grains are less than 250 μm.

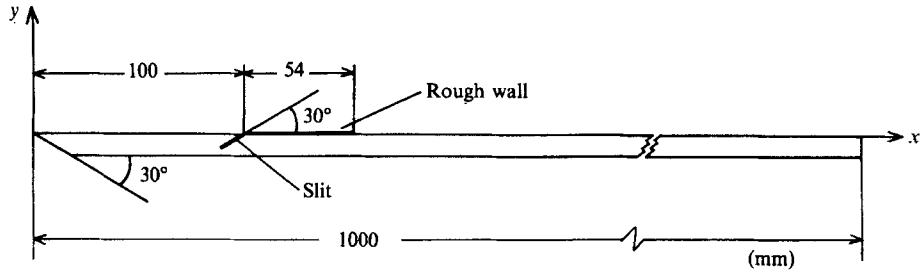

FIGURE 5. Flat plate with a slit for flow visualization at 100 mm from the leading edge. The wall is covered by grains 54 mm in width downstream of the slit.

The experiment was performed at wind velocities up to $U = 5$ m/s. The turbulence level of the main stream was less than 0.08%, and the roughness Reynolds number ranges between 33.3 and 83.3.

Kerosene vapour for flow observation was released from the slit; in the absence of the grains the vapour was transported as a uniform film along the wall. As mentioned above, it is necessary to ensure that the slit does not disturb the flow, but strictly speaking the flow will temporarily separate at the slit and a disturbance due to this separation is unavoidable. Therefore it is so designed that a disturbance at the slit, if ever it occurs, can be absorbed into the random disturbance downstream of the slit caused by grains.

Figure 6 illustrates longitudinal streaks emerging on the flat plate as photographed in this experiment. The Reynolds number at the downstream end of surface roughness referring to the distance from the leading edge was less than 5×10^4, showing that the natural flat-plate boundary layers are sufficiently stable. A periodic phenomenon apparently resulting from the surface roughness was recognized. In view of the observations that (i) the streaks are very regularly spaced with the spacing tending to widen with an increase in the wind velocity and that (ii) the periodic dimension (3–4 mm) differs from the grain diameters, it is likely that the streaks are not produced as wakes of the random surface roughness elements. Thus this phenomenon is one which ought to be considered as related to the turbulence within the boundary layer caused by the surface roughness.

Figure 7 illustrates an example of a boundary layer developing downstream of the roughness for $U = 5$ m/s, where θ indicates the momentum thickness. There is little variation in $\bar{u}/U$ and $\bar{v}/U$, which means that this phenomenon differs from generation of longitudinal vortices due to $\partial\bar{v}/\partial x$ as stated in the previous paper (Aihara *et al.* 1985). It is seen from figure 8 that u' is strongly induced by the surface roughness and v' is proportional to U. Under this experimental condition it is supposed that since the maximum values of disturbances within the boundary layer tend to decay downstream, the longitudinal vortices generated in the sublayer are not amplified enough to contribute to the energy for turbulence, correspondingly that Reynolds number based on the maximum grain diameter, roughness Reynolds number, is in the admissible range (Schlichting 1968). Therefore the experiment is done in the range where the equilibrium of the turbulent boundary-layer through formation of longitudinal vortices is not yet attained. The experimental conditions are convenient for comparison with the analysis in §2. The measured values of $|k|$ and σ about definitely regular longitudinal streaks are shown in figure 2, where $|k|$ is given as the average of three values obtained at a value of y halfway between the position of a maximum value of $(\overline{v'^2})^{\frac{1}{2}}/U$ and the wall. The experimental value falling in the

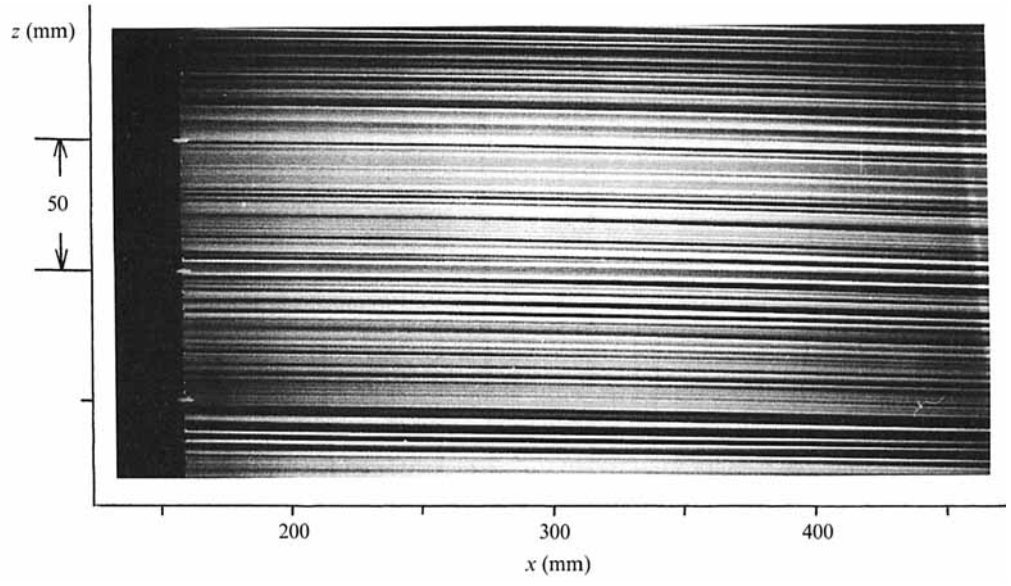

FIGURE 6. Flow visualization of the surface patterns. Longitudinal streaks are regularly spaced in the sublayer. Roughness Reynolds number is 83.3. Flow is from left to right.

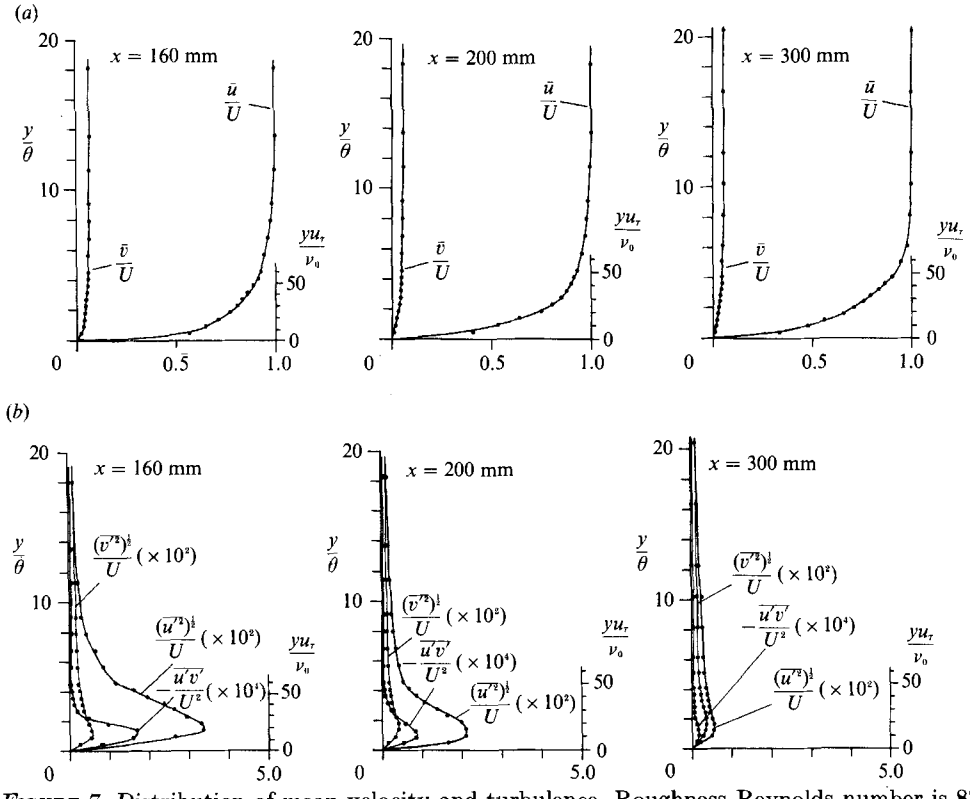

FIGURE 7. Distribution of mean velocity and turbulence. Roughness Reynolds number is 83.3. (*a*) $\bar{u}/U$ and $\bar{v}/U$. (*b*) $(\overline{u'^2})^{\frac{1}{2}}/U$, $(\overline{v'^2})^{\frac{1}{2}}/U$ and $\overline{u'v'}/U^2$.

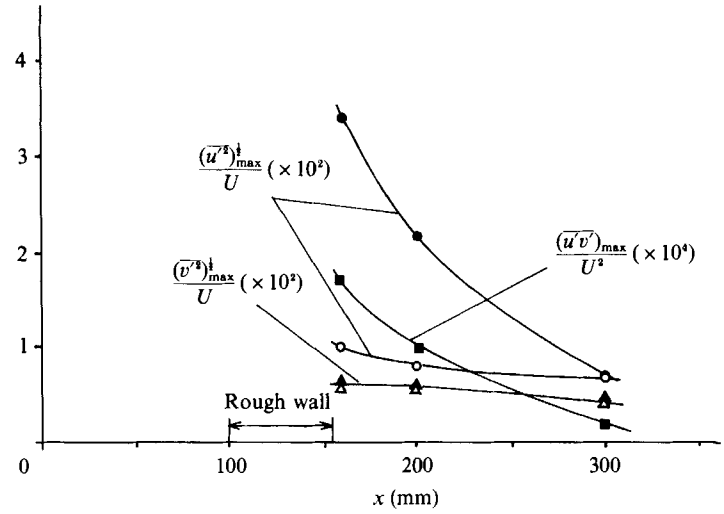

FIGURE 8. Decay of maximum intensity of turbulence in the downstream direction. ○, △, U = 2 m/s, roughness Reynolds number = 33.3; ●, ▲, ■, U = 5 m/s, roughness Reynolds number = 83.3.

instability region is obtained for $U = 5$ m/s, $x = 160$ mm (just downstream of roughness), while the other experimental values on the stable side have been obtained for $U = 3$, 4, 5 m/s, $x = 200$ mm. It is seen that as the turbulence downstream decays, correspondingly the longitudinal vortices also decay and shift to the stable region.

In (1)′, $\partial(\overline{u'v'})/\partial x$ is ignored as being sufficiently small as compared with $\overline{\partial v'^2}/\partial y$ under equilibrium of a mean flow. This is true with a fully developed flat-plate turbulent boundary layer. In the case of an experiment as described in §3, however, at the downstream end of the surface roughness where an artificial disturbance terminates in a discontinuity, $|\overline{u'v'}|$ rapidly decays downstream as illustrated in figure 8. Thus in this case $\partial(\overline{u'v'})/\partial x$ is comparable to $\overline{\partial v'^2}/\partial y$ and influences the dynamic instability of longitudinal vortices. As evident from the figure, $\partial(\overline{u'v'})/\partial x$ is positive and accordingly, when this effect is added to the left-hand side of (1)′, the formation of the longitudinal vortices in the sublayer will be promoted and in consequence the instability region in figure 2 based on (1)′ is expected to spread just downstream of the surface roughness. Indeed regular longitudinal streaks can be recognized in the present experiment in spite of some of the experimental conditions ($U \leqslant 5$ m/s, $x =$ 200 mm) being in the stability region of figure 2; this is supposed to be due to the influence of $\partial(\overline{u'v'})/\partial x$ just downstream of the surface roughness.

As noted in §2.2, $\overline{u'v'}$ can be modelled as

$$-\overline{u'v'} = \nu' \frac{\partial \bar{u}}{\partial y}. \tag{18}$$

Therefore, if we suppose that ν' varies mainly in the y-direction, we get

$$\frac{\overline{\partial u'v'}}{\partial x} = \nu' \frac{\partial}{\partial y}\left(\frac{\partial \bar{v}}{\partial y}\right), \tag{19}$$

and in the same way as in the turbulence model of $\overline{v'^2}$, we recognize the importance of $\bar{v}(y)$ in this case, too. It should be noted that $\overline{u'v'}$ plays an important role, when the third term of the left-hand side in (1) becomes of the same order of magnitude as

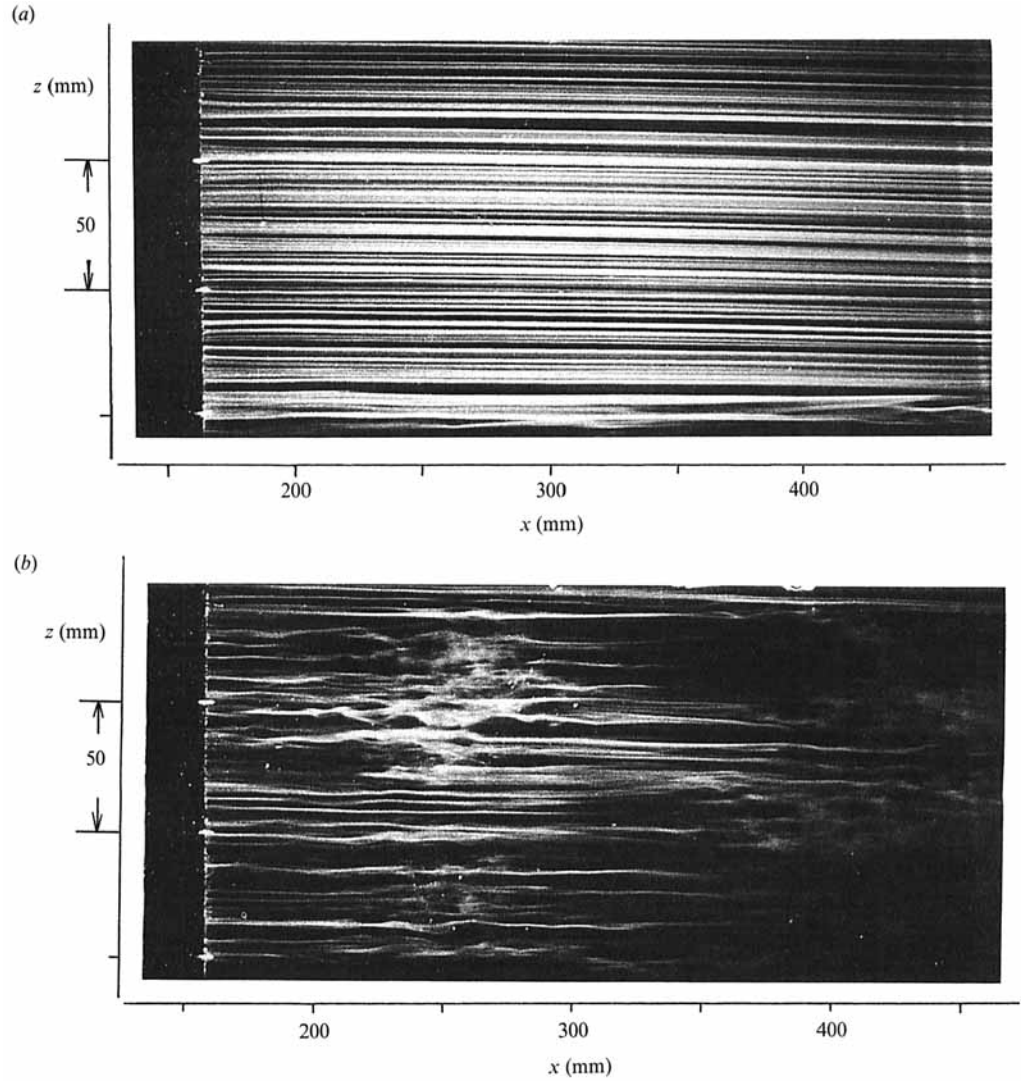

FIGURE 9. Flow visualization of the surface pattern. (*a*) Longitudinal streaks are regularly spaced in the sublayer. $U = 4$ m/s. Roughness Reynolds number is 133. (*b*) Transitional flow. $U = 5$ m/s. Roughness Reynolds number is 167.

the fourth term. Under the state to which Görtler's version applies, which is the assumption of the present analysis, the streamwise derivative is excluded, and the equilibrium of (1)′ is considered important.

3.2.2. *Transitional flow*

Now preliminary results obtained similarly using the JIS-specified no. 36 abrasive grains (diameter less than 500 μm) are to be described. In this case the boundary layer becomes transitional in the range of $U = 4$ m/s to 5 m/s under the effect of surface roughness; the corresponding roughness-Reynolds-number range is 133–167. In figure 9(*a*) at $U = 4$ m/s, it is seen that in spite of larger surface roughness, the periodic streak spacing is almost the same as in figure 6. At $U = 5$ m/s (figure 9*b*), the streaks become unsteady and it is seen that the width in the z-direction is far larger

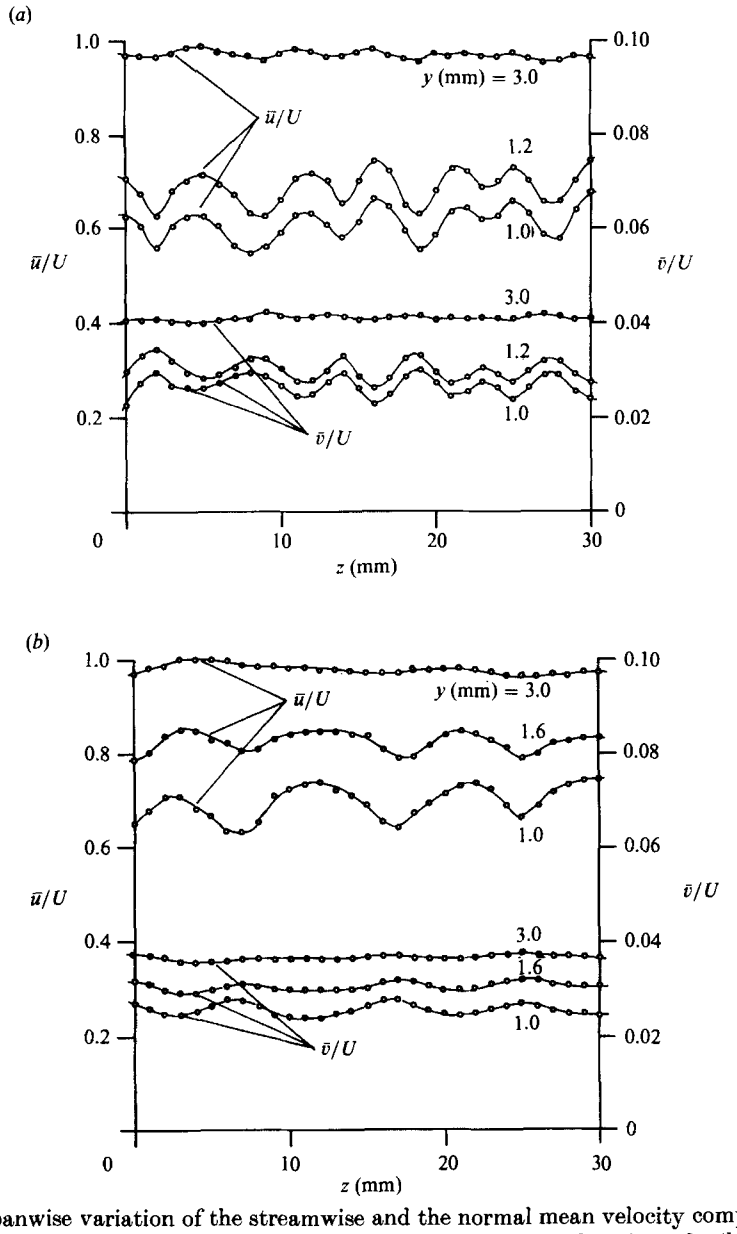

FIGURE 10. Spanwise variation of the streamwise and the normal mean velocity components, $\bar{u}/U$ and $\bar{v}/U$. $x = 170$ mm. (*a*) $U = 4$ m/s. Roughness Reynolds number is 133. (*b*) $U = 5$ m/s. Roughness Reynolds number is 167.

than the earlier streak spacing. Referring to figure 9(*a*, *b*), the z-direction periodicity due to vortices is shown in figure 10(*a*, *b*). It is apparent that in the state of energy being supplied from longitudinal vortices to the disturbance, the longitudinal vortices have a large wavelength and σ is small, which qualitatively agrees with the feedback mechanism as speculated from the linear theory. Eigenvalues at $U = 5$ m/s entered in figure 2 will fall into the instability zone, presenting no conflict with the analysis.

Figure 11 shows a streamwise change of the disturbance. At $U = 4$ m/s, it is seen,

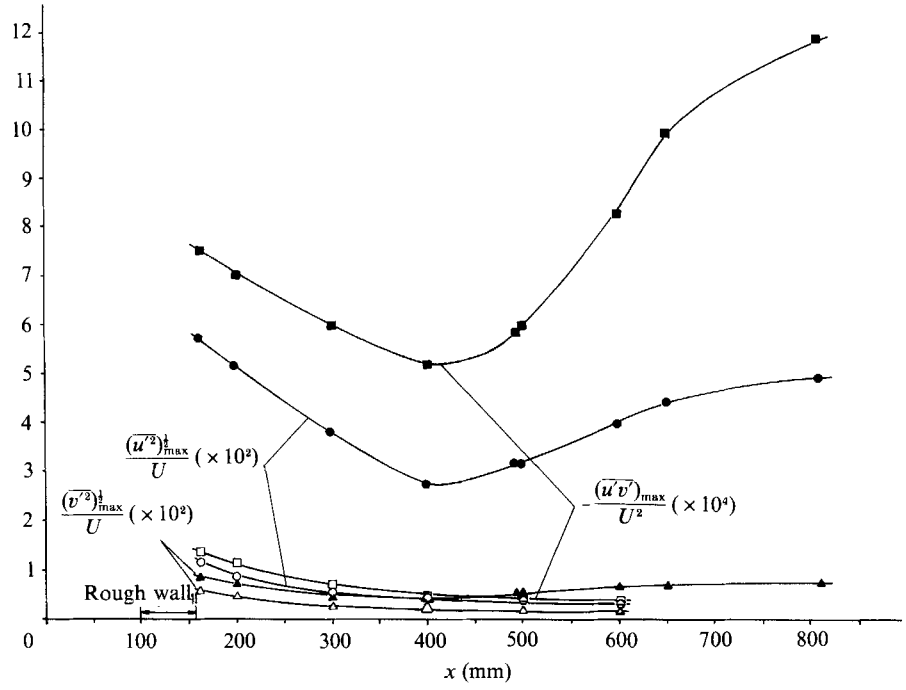

FIGURE 11. Variation of maximum intensity of turbulence in the downstream direction in the transitional flow. ○, △, □, $U = 4$ m/s, roughness Reynolds number = 133; ●, ▲, ■, $U = 5$ m/s, roughness Reynolds number = 167. $x = 600$ mm, $y = 0.8$ mm.

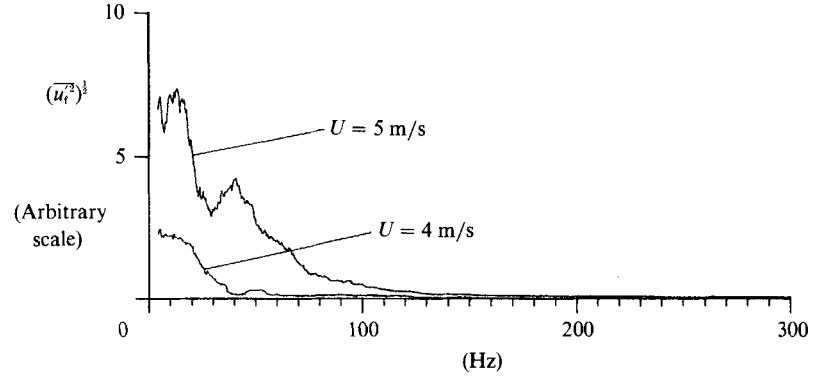

FIGURE 12. Comparison of spectral distributions of u' before ($U = 4$ m/s) and after ($U = 5$ m/s) the transition.

the disturbance attenuates in the x-direction, but at $U = 5$ m/s, it attenuates up to $x = 400$ mm, but thereafter it begins to amplify.

Meanwhile, figure 12 shows spectral distributions of u' at $U = 4$ m/s, $x = 600$ mm and at $U = 5$ m/s, $x = 600$ mm for comparison. The peak appearing around 40 Hz at $U = 5$ m/s is considered to be associated with the unsteadiness of the flow; it seems to correspond to bursting. This suggests that there is an inherent time constant for the feedback loop. After the bursting appears, the flow field becomes complicated owing to the interaction between the turbulence from the roughness and that in the longitudinal vortices. Detailed experiments in the turbulence zone are beyond the scope in the present paper.

4. Discussion of longitudinal vortices from the viewpoint of the thermodynamics of irreversible processes

The theme of the present paper is to investigate the process of achieving a nonlinear equilibrium including turbulence. It is therefore considered necessary to provide a reasonable explanation about why in such a field the longitudinal vortices constitute an object of study. Such a complex flow should be analysed by using the Navier–Stokes equations but it is practically difficult. Instead, the thermodynamics of irreversible processes will here be introduced to obtain a general view of the flow field. The introduction of the thermodynamics of irreversible processes is expected to relate the present problem to the newly developed science of dissipative structures (Glansdorff & Prigogine 1971).

A change of entropy s per unit volume of a fluid can be expressed by

$$\rho T \frac{\mathrm{D}s}{\mathrm{D}t} = \Phi, \tag{20}$$

where the left-hand side shows the Euler derivative of s multiplied by constant temperature T and ρ, and Φ is the dissipation function. Transformation of Φ yields:

$$\rho T \frac{\mathrm{D}s}{\mathrm{D}t} = -2\nu_0 \nabla^2 p + \mu\omega^2, \tag{21}$$

where μ and ω are the viscosity and the three-dimensional vorticity vector respectively. Equation (21) shows that the change of s can be expressed using the so-called flow term (the first term on the right-hand side) and the production term in the quadratic form (the second term on the right-hand side), whereby the condition for a thermodynamically quasi-equilibrium stationary state for an open system is that the entropy production rate is minimum (Glansdorff & Prigogine 1971). Then the time-averaged (21) is integrated from an arbitrary x_1 to x_2 in the x-direction and from the wall ($y = 0$) to ∞ in the y-direction with the assumption of two-dimensionality on the average in the z-direction. Thus the left-hand side gives the net entropy flux to this region, i.e. the net entropy production rate. Meanwhile, the first term on the right-hand side is the integration of $-2\nu_0 \partial\overline{p}/\partial y$ on the wall surface according to Gauss' Theorem and the second term gives the entropy production rate due to vorticity in this region. The vorticity of the mean flow is larger as the flow comes closer to the wall and the disturbance of vorticity due to its unsteady release is also dominant close to the wall. As can be seen from (21), the vorticity of the fluid motion in the boundary layer increases the entropy and at the same time controls $\partial\overline{p}/\partial y$ so as to sustain the rate of the entropy increase at a low level. Mechanically, it is important to find the process whereby the distribution of vorticity $\partial\overline{p}/\partial y > 0$ can be obtained and the entropy production rate is decreasing. Namely, we should discuss the reduction of the degree of freedom in vortices in connection with $\partial\overline{p}/\partial y > 0$ near the wall surface.

Supposedly the most plausible situation will be such that longitudinal vortices are formed and develop near the wall surface. The static pressure p at each vortex centre is lower, as the vorticity increases, with the result that a positive value of $\partial\overline{p}/\partial y$ can be obtained. Referring to (1)′, it can be understood that the condition of $\partial\overline{p}/\partial y > 0$ close to the wall surface will also reduce the instability of the flow. Meanwhile, unlike the other types of vortices, the longitudinal vortices stay longer near the wall with a persistent effect and the axial component of vorticity makes no direct influence on the frictional resistance of the wall. From this behaviour, the relationship between

boundary-layer turbulence and the formation of longitudinal vortices close to the wall can be considered to represent the response of the flow in order to maintain the equilibrium of a turbulent boundary layer.

5. Conclusions

The dynamic instability of the sublayer due to turbulence normal to the wall surface is analysed using a turbulence model. As a result the possibility of longitudinal vortices being formed in the sublayer is deduced. Thus considering the previous experiments which clarified the energy supply of longitudinal vortices to the turbulence field, a feedback loop showing the equilibrium attained in the turbulent boundary layer is derived. The present analysis is applicable to a general boundary layer involving a disturbance, and therefore it may also provide an explanation for the three-dimensionalization accompanying an amplification of a small two-dimensional disturbance within a laminar boundary layer. When a random disturbance is introduced into a boundary layer, regular longitudinal vortices are observed in the sublayer. The relationship between the intensity of turbulence and the spatial wavenumber of the longitudinal vortices is consistent with the results of analysis. The relation between the boundary-layer turbulence and the regular longitudinal vortices in the sublayer is reasonably explained by the thermodynamic argument for the irreversible processes.

Pertaining to the feedback mechanism, we have discussed in §2 the relation between the turbulence intensity and the wavelengths of longitudinal vortices using available knowledge for the turbulence from longitudinal vortices in the sublayer; and in §4 the relation between the intensity of longitudinal vortices and $\partial\bar{p}/\partial y$. Both discussions reveal the primary importance of $\partial\bar{p}/\partial y$ near the wall for the equilibrium of a turbulent boundary layer. As the discussion in §4 is based on a nonlinear analysis, the result shows not only the importance of $\partial\bar{p}/\partial y$ in the linear stability analysis, but also the relation between the amplified longitudinal vortices and resultant positive $\partial\bar{p}/\partial y$. It would be reasonable to consider that a multiple feedback mechanism or self-organization is in operation in the turbulent boundary layer (Haken 1978).

The author would like to express his thanks to Mr H. Koyama, Department of Aeronautics, Faculty of Engineering, University of Tokyo, for his continuous efforts throughout this research.

REFERENCES

Aihara, Y. & Koyama, H. 1981*a* Secondary instability of Görtler vortices – formation of periodic three-dimensional coherent structure. *Trans. Japan Soc. Aero. Space Sci.* **24**, 78.

Aihara, Y. & Koyama, H. 1981*b* Nonlinear development and secondary instability of Görtler vortices. In *Stability in the Mechanics of Continua* (ed. F. H. Schroeder), p. 345. Springer.

Aihara, Y. & Koyama, H. 1982 Three-dimensional turbulent boundary layer along a concave wall. In *Three-Dimensional Turbulent Boundary Layers* (ed. H. H. Fernholz & K. Krause), p. 210. Springer.

Aihara, Y., Tomita, Y. & Ito, A. 1985 Generation, development and distortion of longitudinal vortices in boundary layers along concave and flat plates. In *Laminar–Turbulent Transition* (ed. V. V. Kozlov), p. 447. Springer.

Benny, D. J. & Lin, C. C. 1960 On the secondary motion induced by oscillations in shear flow. *Phys. Fluids* **3**, 656.

BLACKWELDER, R. F. & ECKELMANN, H. 1979 Streamwise vortices associated with the bursting phenomenon. *J. Fluid Mech.* **94**, 577.

BROWN, G. L. & THOMAS, A. S. W. 1977 Large structure in a turbulent boundary layer. *Phys. Fluids* **20**, (10) S 243.

CANTWELL, B. J. 1981 Organized motion in turbulent flow. *Ann. Rev. Fluid Mech.* **13**, 457.

COLES, D. 1978 A model for flow in the viscous sublayer. In *Workshop on Coherent Structure of Turbulent Boundary Layers*, p. 462. Lehigh University.

CORINO, E. R. & BRODKEY, R. S. 1969 A visual investigation of the wall region in turbulent flow. *J. Fluid Mech.* **37**, 1.

FINLAYSON, B. A. 1972 The Method of Weighted Residuals and Variational Principles. Academic.

GLANSDORFF, P. & PRIGOGINE, L. 1971 *Thermodynamic Theory of Structure, Stability and Fluctuations*. Wiley-Interscience.

GÖRTLER, H. 1940 Über eine dreidimensionale Instabilität laminarer Grenzschichten an konkaven Wänden. *Nachr. Ges. Wiss. Göttingen*, New Ser. 2, no. 1.

GÖRTLER, H. & WITTING, H. 1958 Theorie der sekundären Instabilität der laminaren Grenzschichten. In *Boundary Layer Research* (ed. H. Görtler), p. 110. Springer.

GREENSPAN, H. P. & BENNY, D. J. 1963 On shear-layer instability, breakdown and transition. *J. Fluid Mech.* **15**, 133.

KIM, H. T., KLINE, S. J. & REYNOLDS, W. C. 1971 The production of the wall region in turbulent flow. *J. Fluid Mech.* **50**, 133.

HAKEN, H. 1978 *Synergetics*. Springer.

KLEBANOFF, P. S. 1955 Characteristics of turbulence in a boundary layer with zero pressure gradient. *NACA Rep.* 1247.

KLEBANOFF, P. S., TIDSTROM, K. D. & SARGENT, L. M. 1962 The three-dimensional nature of boundary-layer instability. *J. Fluid Mech.* **12**, 1.

KLINE, S. J., REYNOLDS, W. C., SCHRAUB, F. A. & RUNDTADLER, P. W. 1967 The structure of turbulent boundary layers. *J. Fluid Mech.* **30**, 741.

LAUNDER, B. E. & SPALDING, D. B. 1972 *Mathematical Models of Turbulence*. Academic.

PRANDTL, L. 1925 Über die ausgebildete Turbulenz. *Z. angew. Math. Mech.* **5**, 136.

PRATURI, A. K. & BRODKEY, R. S. 1978 A stereoscopic visual study of coherent structures in turbulent shear flow. *J. Fluid Mech.* **89**, 251.

RAO, K. N., NARASIMHA, R. & NARAYANAN, M. A. B. 1971 Bursting in a turbulent boundary layer. *J. Fluid Mech.* **48**, 339.

SCHLICHTING, H. 1968 *Boundary Layer Theory*. McGraw-Hill.

SWEARINGEN, J. D. & BLACKWELDER, R. F. 1987 The growth and breakdown of streamwise vortices in the presence of a wall. *J. Fluid Mech.* **182**, 225.

TAYLOR, G. I. 1923 Stability of a viscous liquid contained between two rotating cylinders. *Phil. Trans. R. Soc. Lond.* A **223**, 289.

TERADA, T. 1928 Some experiments on periodic columnar formation of vortices caused by convection. *Tokyo Imperial Univ. Aero. Res. Inst. Rep.* **3** (31).

WILLMARTH, W. W. & LU, S. S. 1972 Structure of the Reynolds stress near the wall. *J. Fluid Mech.* **55**, 65.